Effects of Tibialis Anterior and Posterior Synergy Perturbations on Multi-Joint Foot Kinematics at Heel Strike

Niharika B. Pathare[1], Anthony H. Le[2], Amy L. Lenz[1]
[1]Dept. Of Mechanical Engineering [2]Dept. of Biomedical Engineering, University Utah, Salt Lake City, UT
Email of Presenting Author: niharika.pathare@utah.edu

Disclosures: None

INTRODUCTION: Coordinated activation of functionally grouped muscles, known as muscle synergy, is critical in maintaining foot–ankle stability during gait, yet its specific influence on segmental foot kinematics during early stance remains insufficiently characterized. At heel strike, synergies among tibialis anterior (TA), tibialis posterior (TP), flexors, and extensors regulate initial foot contact, medial arch stability, and hindfoot alignment. Disruption of these patterns, as observed in post-stroke foot drop or cerebral palsy, can lead to uncontrolled plantarflexion or result in hindfoot valgus and arch collapse due to weak TA or TP dysfunction. Modern robotic simulators can reproduce physiological foot–ankle motion in vitro through cadaveric testing under realistic loading [1,2]. Thus, using a tendon force actuation system, we simulated TA/TP muscle synergy disruptions observed in common neuromuscular foot pathologies and investigated how isolated and combined TA/TP dysfunctions affect multi-joint foot and ankle kinematics at heel strike.

METHODS: Four fresh-frozen male cadaveric lower limb specimens (tibial plateau to toe-tip; 58.8 ± 12.7 yrs, 78.1 ± 16.8 kg) were tested under IRB approval using a 6-DOF robotic gait simulator (FANUC M-20iA) with an integrated 6-axis load cell. Six linear actuators (Unimotion) with in-line load cells (Futek) were used to simulate targeted muscle synergies in six extrinsic tendons: TA, TP, extensors, flexors, peroneals (brevis and longus), and Achilles (Fig. 1). Tendon forces at heel strike were derived using Computed Muscle Control (CMC) on OpenSim's Rajagopal model [3], scaled to those at 20% of the body weight for each specimen, and applied to the six tendons using PID control. For each specimen, the robot's tool center was set to the tibiotalar joint center, about which the tibia was rotated 12° while maintaining a heel strike pose; the limb was then lowered on a force plate (AccuGait, AMTI) until a vertical ground reaction force equal to 20% body weight was reached. Anatomical local coordinate systems (LCSs) for all bones were defined using AAFACT [4]. Five synergy conditions were tested in three trials: All tendons at 100% of the scaled OpenSim-based heel strike forces (Baseline), 50% TA deficit (Condition 1), 50% TP deficit (Condition 2), 50% TA deficit with 120% TP for compensation (Condition 3), and co-contraction of TA and TP at 110% (Condition 4). Bone-mounted infrared marker clusters (Optotrak Certus, NDI) were used to track tibia, fibula, talus, calcaneus, navicular, and cuboid at 250 Hz. Joint angles were computed according to prior published protocols, which involved marker–to–bone LCS transformation (Mimics/3-Matic) and implementing joint-specific Cardan sequences for Euler angle decomposition in the sagittal, coronal, and transverse anatomical planes [5]. All rotations were expressed relative to the proximal bone's LCS. Non-parametric statistical analysis was performed using Friedman tests with Holm-corrected post-hoc Wilcoxon signed-rank tests (α = 0.05), and effect sizes were calculated using rank-biserial correlation (r) to assess biomechanical relevance (R 4.5.1, RStudio, Posit).

RESULTS: Friedman analysis revealed significant effects of synergy conditions at the subtalar sagittal- ($\chi^2(3)=8.1$, p=0.044) and coronal-plane rotation ($\chi^2(3)=10.2$, p=0.017), talonavicular sagittal- ($\chi^2(3)=10.8$, p=0.013), coronal- ($\chi^2(3)=11.1$, p=0.011) and transverse-plane rotation ($\chi^2(3)=9.3$, p=0.026), and tibiotalar sagittal-plane rotation ($\chi^2(3)=12.0$, p=0.007). No Holm-corrected post-hoc comparisons reached significance; however, several pairwise comparisons showed large effect sizes ($r \geq 0.8$; max r = 0.913), particularly in the talonavicular joint (Fig. 2). Relative to baseline heel strike, TA deficit decreased subtalar (–0.65° [–0.82 to –0.49°]) and talonavicular inversion (–0.91° [–1.13 to –0.65°]) while reducing tibiotalar dorsiflexion (–2.27° [–2.61 to –1.96°]). TP compensation further reduced tibiotalar dorsiflexion (–2.37° [–2.64 to –2.14°]) without fully mitigating coronal-plane instability at the subtalar (–0.72° [–0.90 to –0.56°]) and talonavicular joints (–1.06° [–1.25 to –0.84°]). TP deficit produced minimal deviations from baseline in the subtalar joint (sagittal: (0.11° [0.1–0.19°]); coronal: (–0.01° [–0.12 to 0.11°]), while reducing talonavicular dorsiflexion (–0.46° [–0.64 to –0.27°]) and inversion (–0.17° [–0.30 to –0.05°]). In contrast, TA and TP co-contraction increased talonavicular dorsiflexion (+0.75° [0.54–0.98°]) and inversion (+0.46° [0.27–0.65°]), along with subtalar dorsiflexion (+0.61° [0.45–0.77°]) and inversion (+0.24° [0.08–0.41°]). Notably, the talonavicular joint showed positive transverse-plane rotation with respect to baseline under reduced TP forces (+0.19° [0.1–0.57°]) as well as high TP forces during co-contraction (+0.61° [0.5–0.81°]).

DISCUSSION: The observed joint-specific patterns suggest that TA deficits compromise both coronal- and sagittal-plane stability at the subtalar and talonavicular joints. Meanwhile, only 20% additional compensatory TP force may be insufficient to restore healthy kinematics in both planes. This supports the concept of functional compartmentalization in foot muscle synergies wherein dorsiflexor and invertor have distinct roles in maintaining foot-ankle kinematics. The pronounced talonavicular sensitivity, reflected by multiple high effect sizes, emphasizes its function in midfoot stability, consistent with prior in-vitro evidence of mediolateral decoupling [6]. Study limitations include the quasi-static heel-strike protocol, small and homogeneous sample, and selective actuation of key dorsiflexor/invertor tendons. Future research should incorporate additional muscle groups, dynamic loading, and a broader demographic to improve generalizability.

Table 1: Mean TA and TP tendon forces and resulting median differences from baseline in Euler angles for significant joint axes (p* < 0.05) for each synergy

Condition	Tendon force (N)		Median differences in angle from baseline (degrees)					
	TA	TP	Tibiotalar	Talonavicular			Subtalar	
			Sagittal	Sagittal	Coronal	Transverse	Sagittal	Coronal
Baseline	121.91 ± 52.19	10.67 ± 4.57	–	–	–	–	–	–
1	60.95 ± 26.09	10.67 ± 4.57	−2.27	−0.69	−0.91	−0.72	0.3	−0.65
2	121.91 ± 52.19	5.33 ± 2.28	−0.36	−0.46	−0.17	0.19	0.11	−0.01
3	60.95 ± 26.09	12.80 ± 5.48	−2.37	−0.74	−1.06	−0.71	0.38	−0.72
4	134.10 ± 57.41	11.73 ± 5.02	0.09	0.75	0.46	0.61	−0.11	0.24

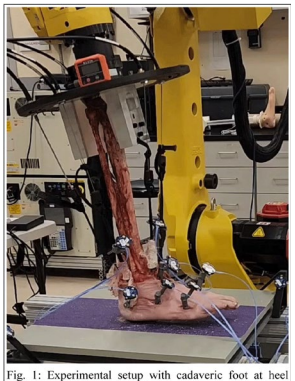

Fig. 1: Experimental setup with cadaveric foot at heel strike: Each tendon is sutured to a stiff sleeve and linked to linear actuator via cable. Tibia is rigidly fixed to the robot end-effector via a custom fixture, allowing free fibular motion. Optical markers are mounted on custom-designed bone pins.

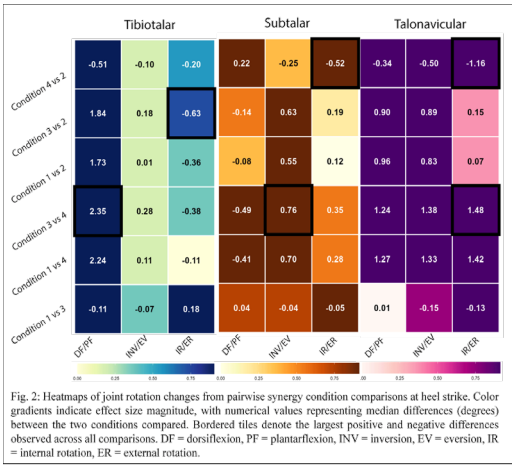

Fig. 2: Heatmaps of joint rotation changes from pairwise synergy condition comparisons at heel strike. Color gradients indicate effect size magnitude, with numerical values representing median differences (degrees) between the two conditions compared. Bordered tiles denote the largest positive and negative differences observed across all comparisons. DF = dorsiflexion, PF = plantarflexion, INV = inversion, EV = eversion, IR = internal rotation, ER = external rotation.

SIGNIFICANCE/CLINICAL RELEVANCE: Foot drop and flatfoot deformity often stem from TA–TP dysfunction, yet their direct impact on joint-level kinematics has been poorly defined. By identifying the talonavicular joint's high sensitivity to TA–TP synergy disruption, this study highlights a critical target for interventions such as orthoses, tendon transfers, or stimulation therapies to restore stability at heel strike.

REFERENCES: [1] Ledoux WR. 2023. Foot Ankle Clin 28:45–62. [2] Baxter JR. 2016. J Orthop Res 34:1663–1668. [3] Rajagopal A. 2016. IEEE Trans Biomed Eng 63:2068–2079. [4] Peterson AC. 2023. Front Bioeng Biotechnol 11:1255464. [5] Le AH. 2025. J Biomech 186:112740. [6] Burg J. 2013. Gait Posture 38:56–61.